Observation of intercalation of excess oxygen in Bi2Sr2CaCu2O8+y single crystal

G. S. Shekhawat, Ram P. Gupta, A. Agarwal, P. D. Vyas, P. Srivastava, N. L. Saini, S. Venkatesh, and K. B. Garg

---

Articles you may be interested in

Broadly tunable, high-power terahertz radiation up to 73K from a stand-alone Bi2Sr2CaCu2O8+ δ mesa
Appl. Phys. Lett. **105**, 202603 (2014); 10.1063/1.4902336

Reinforced fluropolymer nanocomposites with high-temperature superconducting Bi 2 Sr 2 CaCu 2 O y
AIP Conf. Proc. **1620**, 582 (2014); 10.1063/1.4898301

Resistive switching behaviors in Bi2Sr2CaCu2O8+d (Bi-2212) stacks
J. Appl. Phys. **109**, 07E147 (2011); 10.1063/1.3562521

Magnetic flux oscillations in partially irradiated Bi 2 Sr 2 CaCu 2 O 8 + δ crystals
J. Appl. Phys. **105**, 07E310 (2009); 10.1063/1.3068647

Oxygen loss effect under both reducing and oxidizing thermal treatments on superconductivity of singlecrystal Bi2Sr2CaCu2O8+y
J. Appl. Phys. **76**, 595 (1994); 10.1063/1.357050

Observation of intercalation of excess oxygen in $Bi_2Sr_2CaCu_2O_{8+y}$ single crystal

G. S. Shekhawat, Ram P. Gupta, A. Agarwal, and P. D. Vyas
Central Electronics Engineering Research Institute, Pilani-333031 Rajasthan, India

P. Srivastava, N. L. Saini, S. Venkatesh, and K. B. Garg
University of Rajasthan, Jaipur-302004

Effects arising from the intercalation of excess oxygen in Bi–O layer has been observed at room temperature using atomic force microscopy. The excess oxygen is incorporated by oxygenating the pure sample. The oxygen is trapped between the alternating Bi–O layers along the *b* direction. This leads to a change in the local interatomic bond length along the *b* axis, while the periodicity remained invariant along the *a* axis. In addition, in-plane atomically resolved structure of single crystal has been imaged at room temperature using AFM. The lattice spacings indicate that the observed structure corresponds to the in-plane bismuth and oxygen positions. Furthermore, high-resolution scanning tunneling spectroscopy measurements show that oxygen doping increases the Bi–O layer density of states near the Fermi level giving rise to metallicity, whereas the pure sample reveals a semiconducting energy gap in the tunneling spectrum. © *1995 American Institute of Physics.*

Scanning tunneling microscopy (STM)/scanning tunneling spectroscopy (STS) have been extensively applied to the studies of high temperature superconducting materials (HTSC).[1–6] In particular, the cleaved surface of $Bi_2Sr_2CaCu_2O_{8+y}$ (BSSCO) single crystal has been most frequently subjected to STM/STS studies,[2–5] revealing the *b*-axis modulations superstructure and possible insulating nature of the surface Bi–O mono-layer.[4,5] In STM, the tunneling current is proportional to the integral of the density of states (DOS) from E_F to the bias energy eV_b. Therefore, the STM image is sensitive to the DOS. Most of the studies[4,5] indicate that the ordered square spots in the STM image are bismuth (Bi) atoms. The reason why oxygen is not seen under the STM can then be attributed to the relatively small contribution to the local DOS near the Fermi level from the O $2p$ orbitals.[7,8] In contrast to this, atomic force microscopy (AFM)[9,10] has recently been developed as a new technique for extending the high resolution capabilities of STM. In AFM, the images were obtained by mapping interatomic forces between the AFM tip and the surface of the sample. Usually, it can be considered that interatomic forces have two components: one originates from interaction between ion cores and the other is associated with valence electrons. Consequently, it is conceivable that AFM and STM might be sensitive to different types of sites on the surface. This is the primary reason behind preferring AFM by us rather than STM to map surface topography on atomic scale. AFM can be applied to nonconducting as well as conducting surfaces.

An important problem that has not been adequately addressed for $Bi_2Sr_2CaCu_2O_{8+y}$ is to understand how the structural as well as electronic states evolve with oxygen doping, since doping finally introduces holes into this system that destroys the insulating state and yields a metallic state.[11] For this purpose the observation of pure and oxygen annealed samples seems to be of great importance. To investigate precisely the effect of oxygen doping on the surface structure as well as the normal density of state, we have used AFM/STS. We report the systematic room temperature measurements on the single crystals of $Bi_2Sr_2CaCu_2O_{8+y}$ for investigating the effects occurring in the nature and the properties of the Bi–O layer on the crystal surface.

Single crystals of $Bi_2Sr_2CaCu_2O_{8+y}$ were grown by the flux technique. Such crystals have a smooth Bi–O plane along which cleavage is easy. For our AFM we used NanoScope II, Digital Instruments, USA. Imaging was done in air. Scanning was done in constant force mode. Images consist of 400 scan lines of 400 pixels each. Typical image acquisition times were 150–200 s per image. The AFM images were taken using a commercial Au-coated 100 μm triangular Si_3N_4 cantilever (force constant≈0.6 N/m). The apparatus was enclosed in an airtight box for reducing the noise due to air turbulence.

For STS observation, initially well-resolved images of Bi–O layer were obtained in the STM mode and subsequently the instrument was switched into the STS mode through the software program. Thus, I–V and $d \ln T/d \ln V$ for a particular layer could easily be acquired as a function of bias voltage (V). Current (I) versus voltage (V) curves were acquired by interrupting the feedback loop and then ramping the sample-tip bias voltage while digitally storing $I(V)$. The I–V data shown in the figures represent an average of 30–40 curves obtained at the selected surface site.

Figure 1(a) displays a typical two-dimensional perspective view of an atomically resolved $Bi_2Sr_2CaCu_2O_{8+y}$ single crystal scanned over an area of 6 nm×6 nm. It is well known that these crystals cleave preferentially along the weakly interacting Bi–O/Bi–O double layers to yield a stable, unreconstructed Bi–O surface that is ideal for surface-sensitive investigations.[12,13] The surface viewed in the AFM image is the Bi–O plane. This is in fact also clear from the interatomic distances shown in Fig. 1(b) which is a cross section profile along a line shown in Fig. 1(a). This is equal to 2.4

FIG. 3. 4×4 nm AFM 3D image of an oxygen-annealed BSCCO single crystal showing intercalation of excess oxygen atoms between alternating Bi–O layers. Bright regions represents maximum height from the surface. The arrows indicating the location of excess oxygen.
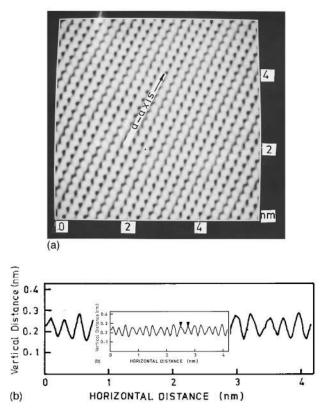
FIG. 1. (a) Top view of 6×6 nm AFM image of BSCCO single crystal obtained using constant force mode. The structure in the image has tetragonal symmetry with a spacing of 2.4±0.02 Å between surface sites. Horizontal streaks are due to a vibrational noise. (b) AFM line scan taken across the line shown in (a). Distances between markers are given in nanometers.

±0.02 Å and is in agreement with the reported Bi–O spacing in the (001) basal plane. These spots define a square lattice that is consistent with the tetragonal symmetry of the crystal.

In the narrow scan images of $Bi_2Sr_2CaCu_2O_{8+y}$, we have observed the atomic chains running along the [010] direction of the corresponding perovskite cell. These chains have a lateral sinusoidal modulation that can be seen in Fig. 2. The distorted structure of the 2212 phase is therefore a typical example of the ''incommensurate superstructure.''
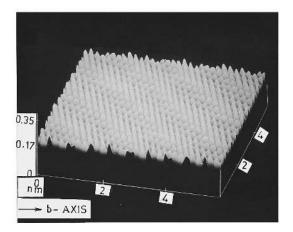

FIG. 2. Narrow scan image that shows the one-dimensional superlattice modulations with a period of 2.5 nm. This image was acquired by recording the Z piezo feedback voltage necessary to keep the force between the surface and the tip constant (constant force mode).

Similar TEM[14,15] and STM[2–6] observation on modulated structure have been reported earlier. The modulation observed in our case is long-range order and it extends up to 600–650 Å comparable to that observed by Kirk et al.[2] The sample studied exhibited this type of modulation effect along one direction (say b axis) and little or no effect in the perpendicular direction (i.e., a axis). The mean value of the modulation period which is of sinusoidal form is found to be 2.5 nm, which compares well with the reported modulation length of 2.6 nm for a pure BSCCO-2212 sample,[2–4] thus indicating that the cleaved surface is the Bi–O plane.[16] Its origin has been ascribed to the atomic mismatch between the rock salt structure of the double Bi–O/Sr–O layers and the perovskite structure formed by the other cations.[16,17]

The AFM image taken on the cleaved surface of oxygenated BSSCO at room temperature is illustrated in Fig. 3. In this figure, one can clearly see the long-range ordering resulting from the oxygen insertion. The oxygen is trapped between the alternating Bi–O layers along the b direction (indicated by arrows in Fig. 3). As may be noticed, the rows of interstitial oxygen atoms running along the a axis (Fig. 3) lead to a change in the local interatomic bond length along the b axis, typically the Bi–O distance along the b axis of the pertinent subunit cell was found to increase from 2.4±0.2 to 3.2±0.04 Å as depicted in Fig. 4(b), while the periodicity remained invariant at 2.4±0.02 Å along the a axis [Fig. 4(a)]. Figure 4 was obtained in the section mode of the NanoScope with the cursor lines aligned, respectively, on the single atomic rows in the two directions.

Apart from observing the intercalation of excess oxygen after alternating Bi–O layers, the modulation period seems to be slightly reduced in oxygenated samples in comparison to that of as-prepared samples. This effect may be due to the peculiar characteristics of the double Bi–O layers, i.e., Bi–O bond length within the plane is smaller in comparison to their relatively large interlayer spacing. As a consequence, these layers serve as an effective sink for excess oxygen, which results in releasing the strain arising from a mismatch in the perovskite layers[17] and lowers the modulation length.
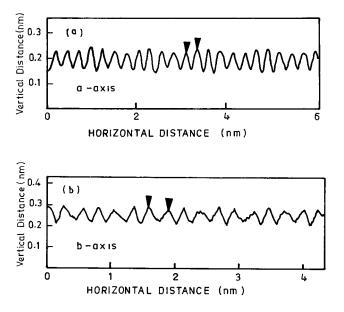
FIG. 4. Variation in bond length of Bi–O resulting from the insertion of excess oxygen atoms: (a) periodicity of 2.4 Å is invariant along the *a* axis as indicated by markers; (b) enhancement in the bond length along the *b* axis after insertion of excess oxygen atoms resulting from oxygenation of pure crystals.

This is in accordance with the results obtained using HRTEM by other workers.[18,19]

In Figs. 5(a)–5(d) we plot the *I* and $d \ln I/d \ln V$ versus bias voltage *V* data obtained on the as-prepared and oxygenated samples, where $d \ln I/d \ln V$ is proportional to the local density of states independent of the tip sample distance.[20] The spectroscopic data were taken at a large bias voltage that corresponds to a relatively large tip-sample separation and thus the results should be representative of the Bi–O layer DOS without the contribution from the CuO$_2$ layer.[5,13] An important result is evident upon comparing the two data of *I*–*V* characteristics near E_F for the pure and the oxygen-annealed samples. The first one exhibits extremely low current within ± 330 mV of E_F and a sharp increase beyond these points, while the latter shows a smooth increase in *T* for even low volt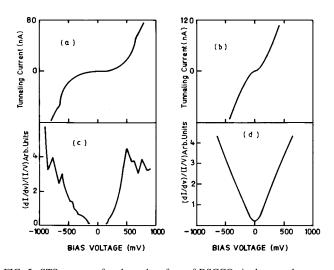ages. Since the tip-sample separation is the same in both the experiments, it is unlikely that this difference is due to a distance scaling effect.

The DOS profile of the normalized conductivity (*V/I*)/(*dI/dV*) shows that there is a 230 meV gap in the Bi–O layer for the pure sample [Fig. 5(c)]. This indicated that the density of states at E_F is negligibly small, suggesting that the Bi–O plane is nonmetallic.[4,5] On the other hand, the zero-bias conductance is finite for an oxygen-annealed sample [Fig. 5(d)], thus indicating that this layer is metallic. This suggests that oxygen doping introduces states in the Bi–O layer near E_F. One explanation for these results is that oxygen doping may cause the Bi–O band to shift and cross E_F, thereby making it metallic.[21,22] Whether the impurity states caused by oxygen or the Bi–O band crosses the Fermi level giving rise to metallicity is still unclear.

In summary, AFM and STS have been used to elucidate the surface as well as low-energy electron states of the Bi–O layer before and after oxygenation of Bi$_2$Sr$_2$CaCu$_2$O$_{8+y}$ single crystals. Our AFM study provides further insight into the changing characteristics of Bi–O layers induced by excess oxygen. The excess oxygen observed is primarily responsible for reduction in the modulation period in the oxygenated sample. Our STS measurements directly demonstrate that oxygen doping increases the Bi–O layer DOS near E_F, thus changing the Bi–O layer from semiconducting to metallic behavior.

FIG. 5. STS spectra of a cleaved surface of BSCCO single crystal.

[1] M. Tanaka, T. Takahashi, H. Katayama-yoshida, S. Yamazaki, M. Fujimami, Y. Okase, W. Mizutani, M. Ono, and K. Kayimura, Nature **339**, 691 (1989).
[2] M. D. Kirk, J. Nogami, A. A. Baski, D. B. Mitzi, A. Kapiltulnik, T. H. Geballe, and C. F. Quate, Science **242**, 1673 (1988).
[3] M. D. Kirk, C. B. Eom, B. Oh, S. R. Spielman, M. R. Beasley, A. Kapitulnik, T. H. Geballe, and C. F. Quate, Appl. Phys. Lett. **52**, 2071 (1988).
[4] C. K. Shih, R. M. Feenstra, and G. V. Chandrasekhar, Phys. Rev. B **43**, 7913 (1991).
[5] T. Hasegawa, M. Nantoh, A. Takagi, H. Ikuta, N. Kawasaki, H. Koinuma, and K. Kitazawa, J. Phys. Chem. Solids **53**, 1643 (1992).
[6] Z. Zhang and C. H. Lieber, Phys. Rev. B **46**, 5845 (1992).
[7] H. Krakauer and W. E. Pickett, Phys. Rev. Lett. **60**, 1655 (1988).
[8] L. F. Mattneiss and D. R. Hamann, Phys. Rev. B **38**, 5012 (1988).
[9] G. Binning, C. F. Quate, and Ch. Gerber, Phys. Rev. Lett. **56**, 930 (1986).
[10] T. R. Albrecht and C. F. Quate, J. Appl. Phys. **62**, 2599 (1987).
[11] G. A. Sawastsky, Nature **342**, 480 (1989).
[12] B. O. Wells, Z. H. Shen, D. S. Dessau, W. E. Spicer, C. G. Olson, D. B. Mitzi, A. Kapitulnik, R. S. List, and A. Arko, Phys. Rev. Lett. **65**, 3056 (1990).
[13] X. L. Wu, Z. Chang, X. L. Wang, and C. M. Lieber, Science **248**, 1211 (1990).
[14] T. M. Shaw, S. P. Shivashanker, J. J. Cuomo, T. R. McGuire, R. A. Roy, K. H. Kelleher, and D. S. Yee, Phys. Rev. B **37**, 9854 (1988).
[15] P. L. Gai and P. Day, Physica C **152**, 335 (1989).
[16] H. W. Zandbergen, W. A. Groen, F. C. Mijlhoff, G. Van Tendeloo, and S. Amolinckx, Physica C **156**, 325 (1988).
[17] H. W. Zandbergen, W. A. Groen, G. Van Tendeloo, J. Van Landuyt, and S. Amelinckx, Solid State Commun. **66**, 397 (1988).
[18] J. M. Tarascon, P. Barboux, G. W. Hull, R. Ramesh, O. H. Green, and M. Groud, Phys. Rev. B **41**, 691 (1990).
[19] W. A. Groen and H. W. Zandbergen, Solid State Commun. **68**, 527 (1988).
[20] R. M. Feenstra, J. A. Stroscio, and A. P. Fein, Surf. Sci. **181**, 295 (1987).
[21] H. Krakauer and W. E. Pickett, Phys. Rev. Lett. **60**, 1665 (1988).
[22] H. S. Hybertsen and L. F. Mattheiss, Phys. Rev. Lett. **60**, 1661 (1988).

Appl. Phys. Lett., Vol. 67, No. 22, 27 November 1995

Shekhawat *et al.* 3345